FIRST STEPS TOWARDS A LANDSLIDE INVENTORY MAP OF THE CENTRAL KARAKORAM
NATIONAL PARK

Contributo dell'autore Maria Teresa Melis

Maria Teresa Melis ha curato la sezione introduttiva legata all'utilizzo del DEM, ha fornito i dati cartografici di base necessari per le analisi e realizzando le cartografie derivate (§Digital elevation Model and its derivatives). Ha infine collaborato alla discussione dei risultati (§Results and discussion).

First steps towards a landslide inventory map of the Central Karakoram National Park

Chiara Calligaris[1*], Giorgio Poretti[1,4], Shahina Tariq[2] and Maria Teresa Melis[3, 4]

[1]Department of Mathematics and Geosciences, University of Trieste, Via Weiss 2, 34128 Trieste, Italy
[2]COMSAT, University of Science and Technology, Park Road, Chak Shahzad, Islamabad, Pakistan
[3]TeleGIs Laboratory, Department of Chemistry and Geology, University of Cagliari, via Trentino 51, 09127 Cagliari, Italy
[4]Ev - K2 - CNR Committee, Via San Bernardino 145, 24126 Bergamo, Italy
*Corresponding author, e-mail address: calligar@units.it

Abstract

The northeastern part of Pakistan is known to be a region of extremes, where the highest reliefs and the longest glaciers of the world may be found. In this environment, through the multidisciplinary *Social, Economic and Environmental Development (SEED) Project* the knowledge of the sustainable exploitation possibilities of the Central Karakoram National Park area (CKNP) will be improved.
One of this project's objectives is the analysis of the geological hazards giving as output a landslide inventory and a susceptibility map, utilizable as functional tools for a future sustainable territorial planning. The Bagrot Valley, chosen as test site, was partially field surveyed and part of the landslide-prone areas preliminarily identified through DEM analysis, GIS techniques and Analytical Hierarchy Process (AHP) methodology, were later validated on the field. ASTER DEM was used as the basis of morphometric analysis.
Keywords: Landslides, Geographical Information System (GIS), susceptibility map, DEM, ASTER.

Introduction

The Central Karakorum National Park (CKNP) region has to be preserved in order to maintain its ecosystem, cultural values and the scenic beauty of the landscape for the benefit of the present and future generations.
The mountain areas and the geological features, with particular rereference to high seismicity, make this region particularly prone to natural hazards. In these regions, earthquakes, landslides, snow avalanches and flash floods are the most common types of geological

hazards, therefore only small portions of the territory are suitable for life and the resident people are, in turn, forced to live in dangerous zones.

In this environment, a multidisciplinary project, named SEED (*Social, Economic and Environmental Development in the CKNP Region Project*) has been developed by the Ev-K2-CNR Committee [2008]. SEED is made up of several different projects, each one focused on a different theme (e.g., glaciology, meteorology, land cover). This multidisciplinary approach permits the characterization of the study area from different points of view. The improved knowledge of the territory focusing on the theme of landslides is one of the SEED project's aims, that could be an important tool for a future sustainable territorial planning. In fact, the SEED project has the general aim to promote the sustainable development of the local communities of the Gilgit-Baltistan Region. In this context, an inventory of landslide bodies and a map of landslide- or rock fall-prone areas [Guzzetti et al., 2012] should be useful to identify the areas where human settlements must be avoided and consequently it provides to the stakeholders an important updatable tool for territorial planning, as required by the new management plan for the national park, where a zoning system for ecosystem conservation and promotion of tourism is recommended.

In order to reach the suggested goal, it was decided to analyze the area through Digital Elevation Models (DEMs) derived from ASTER images (30 m grid cell size), which may be considered a powerful tool for visual and mathematical analysis of the topographic surface at a regional scale [Kamp et al., 2003; Gullà et al., 2008]. These instruments, used in a barren territory, visited only by occasional mountain climbers and porters, are valuable in order to identify landforms and deposits modeled by surface processes. The morphological parameters used for the characterization of the topographic surface are the main derived products of DEMs in remote areas and in areas where no topographic maps are available. A comparative study on the use of different DEMs for terrain analysis is discussed in Ansari et al. [2012]. The authors underline that the use of DEMs, as a tool for geomorphological mapping, landslide, susceptibility/hazard assessment, has got a wide diffusion mainly because they provide the foundation for deriving surface morphological parameters such as slope, aspect, curvature, slope profile and catchment areas. In the review of the applications of remote sensing data for earth surfaces processes analysis Tarolli et al. [2009] highlight the use of ASTER data for geological features extraction [Abrams, 2000] for the evaluation and quantification of sedimentary deposits [Bubenzer and Bolten, 2008] and in the landslide hazard assessment [Fourniadis et al., 2007]. The application of ASTER DEM in the evaluation of landslide susceptibility maps is discussed in Chau et al. [2004], Toutin [2008], Choi et al. [2012], Gokceoglu [2012] and Song et al. [2012]. Moreover, the DEM extracted from ASTER is used in the Artificial Neural Network (ANN) approach for landslide susceptibility mapping, for the generation of geomorphological parameters [Nefeslioglu et al., 2008; Kawabata et al., 2009; Choi et al., 2012].

In this work the interaction of land cover and landslides is analyzed by Peduzzi [2010] on an area of North Pakistan using ASTER DEM for the extraction of landslides susceptibility maps.The landslide susceptibility study [Fell et al., 2008; Van Wasten et al., 2008] was analyzed with the application of the Analytical Hierarchy Process (AHP) [Ayalev et al., 2004; Bajracharya et al., 2008; Komac, 2006; Moradi et al., 2012; Othman et al., 2012;

Phukon et al., 2012] based on the indexing on data layers and parameters as slope angle, slope aspect, slope curvature, geo-lithology, distance to tectonic structures and vegetation [Ruff et al., 2008] since these intrinsic variables determine the susceptibility of landslides [Dahal et al., 2008]. The method was tested in the Bagrot valley, located in the extreme north west of the park. Through the analysis of the DEM, different slope morphologies were pointed out and the main landslides were identified (areas subjected to rock falls, single rock falls and debris flows) [Varnes, 1984].

Research area overview

The 10,000 square kilometers Central Karakoram National Park (CKNP), established in 1993, is the largest park in Pakistan (Fig. 1). It is situated in the Northern Areas (Fig. 1). Approximately 230 villages, 97,608 people and 13,159 households are located in areas adjacent to the CKNP. The area is part of the Asian high-mountain system of Hindukush-Karakorum-West Himalaya that includes Mount K2 (8611 m a.s.l.), the second highest peak in the world. Internationally renowned for mountaineering and trekking opportunities, the park protects the greatest concentration of high mountains on Earth. It includes sixty peaks over 7,000 m, and ten of the world's highest and most famous mountains, including Gasherbrum, Broad Peak and Masherbrum which are located within its boundaries. This cluster of peaks attracts 60 to 70 mountaineering expeditions every year. Located at an elevation above 2,000 m with peaks averaging over 6,000 m, the park is characterized by glacial and periglacial conditions, with glaciers joining to form the largest and most extensive glacial systems outside the polar regions [Ev-K2-CNR, 2008]. The present research is focused on the Bagrot valley area, located in the north-eastern side of Gilgit (Fig. 1). The Bagrot valley has an area of about 374 square kilometers battered by rock falls and debris flows.

Landslide-prone areas identification: methodological approach

The present research is an attempt to produce a landslide susceptibility map, taking advantage of GIS and remote sensing tools [Gardner and Saczuk, 2004; Guzzetti et al., 2012]. A multidisciplinary approach was applied to determine the meaning of event-controlling parameters in triggering the landslides [Kamp et al., 2008; Ruff et al., 2008]. The evaluated parameters [Dahal et al., 2008] included geology, tectonic structures as thrusts and faults, plan curvatures, slope angles, aspect and the drainage net. According to Kamp et al. [2008], there are three steps that need to be taken into account in order to study, with a good accuracy, an area affected by landslides.

The first step involves the implementation of a landslide inventory map, providing the location and outlines of landslides [Spiker and Gori, 2000; Chacon et al., 2006]. The second step consists in the production of a landslide susceptibility map, which includes the spatial distribution of event-controlling parameters, that means that the intrinsic parameters have to be defined and prepared for the GIS analysis. This will allow landslide-prone areas to be defined, independently of temporal controls, and will indicate where landslides may occur in the future [Chacon et al., 2006]. The third step is the production of a landslide hazard map.

Considering the present research started in 2011 in the test area, the first step, was accomplished through field surveys, the second one was realized through the GIS analysis of the geological and DEM data, while the third one is still in progress.
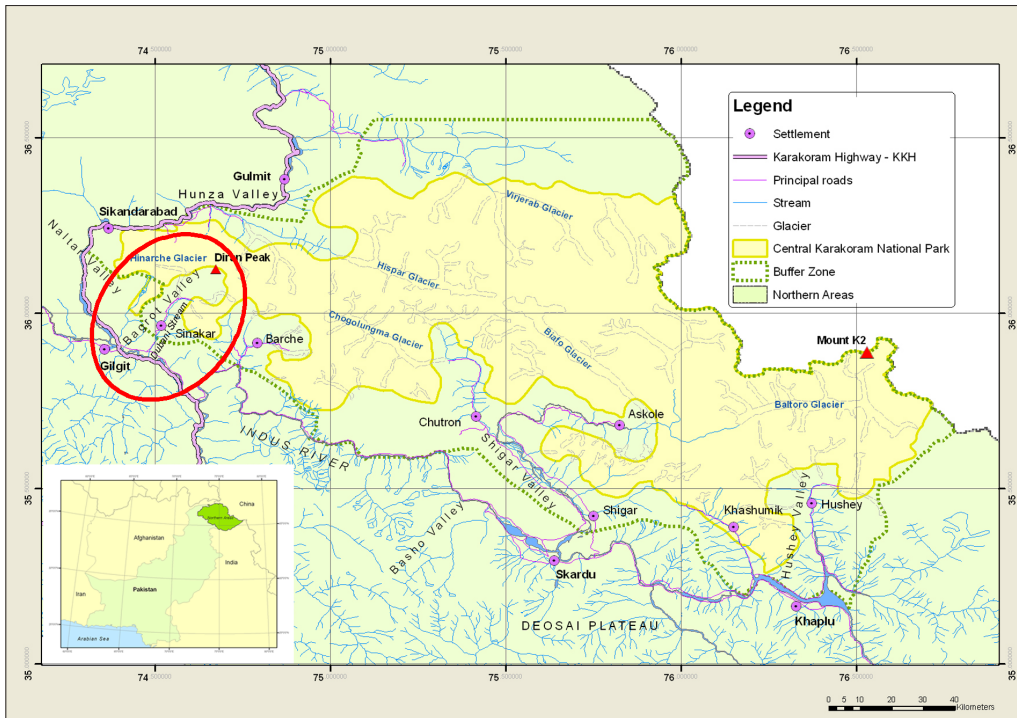
Figure 1 - The CKNP is located in the Northern Areas. Bagrot Valley is the test site area (inside the red ellipse).

The inventory of landslides and their distribution were mapped using the available topographic maps (1:25,000 scale topo-sheet). At first, the geological and lithological conditions were analyzed, than the main geomorphologic parameters (slope angle, aspect and plan curvatures) were extracted from the ASTER images.

The obtained parameters were later combined using the Analytical Hierarchy Process (AHP) method and plotted as output in the landslide-prone area raster map [Ayalew et al., 2004; Komac, 2006; Intarawichian and Dasanada, 2010; Moradi et al., 2012; Phukon et al., 2012]. These preliminary results were validated in the field, using GPS, identifying the main landslides present in the studied area. As for all these types of analyses, the quality of the results is mainly dependent on the DEM resolution [Kamp et al., 2003; Sarkar et al., 2004; Tarolli et al., 2012].

Going into details: a landslide susceptibility map was obtained combining the different factors in accordance with their relative influence to landslide occurrence. The AHP is the methodology that permits to assign a rate not only to the parameters but also to the classes in which each parameter is subdivided [Saaty, 2000]. For the present research the pair-wise comparison matrix presented in Table 2 was used. The considered parameters were arranged in hierarchical order of priorities in rows and columns to generate a pair-wise comparison matrix. At the same time, also the classes in which each parameter has been subdivided were arranged with the same technique using the 9 points defined in Table 1. This method may be defined a Weighted Linear Combination (WLC) where secondary – level weights are opinion-based scores [Ayalew et al., 2004].

Table 1 - Pair-wise comparison table [Saaty, 2000].

Intensity of importance for each considered parameter	Importance definition	Explanatory notes
1	Equal importance	Both parameters contribute equally to the objective
3	Moderate importance	One parameter is considered, based on experience, slightly favoured over another
5	Essential or strong importance	One parameter is strongly favoured over the other
7	Very strong or demonstrated importance	A parameter is very strongly favoured over another
9	Extreme importance	The evidence is favouring a parameter over another
2,4,6,8	Intermediate values between the categories	If and when is needed a compromise

The weights of each parameter were calculated dividing the geometric mean of each row of the matrix by the total of geometric mean in a column of a matrix. The weights were later normalized.

Afterwards ranks and rates were linearly combined (WLC) obtaining the Landslide Potential Index (LPI) according to the formula:

$$LPI = \sum (R_i \times W_{ij}) \quad [1]$$

where $i = 1 - 9$, R_i is the rank for parameter i and W_{ij} is the weight for class j of i factor.

The map obtained as a result of the overlapping weighted raster datasets, represents the distribution of the LPI index values that were later classified into 6 potential landslide susceptibility classes obtaining a landslide susceptibility map (Fig. 4) [Davis, 1986; Sarkar et al., 2004].

The complete list of numerical grades adopted for the present research is summarized in the Tables from 2 to 6.

Table 2 - 1. Slope, 2. Plan curvature, 3. Geology, 4. Distance from drainage, 5. Distance from lineaments, 6. Aspect, 7. Geometric mean, 8. Factor weight.

Parameters	1	2	3	4	5	6	7	8
(1) Slope	1	5	2	6	7	3	3.2864	0.4186
(2) Plan curvature	0.2	1	3	5	7	1	1.6610	0.2116
(3) Geology	0.5	0.33	1	3	5	3	1.3967	0.1779
(4) Distance from drainage	0.16	0.14	0.33	1	2	4	0.6241	0.0795
(5) Distance from lineaments	0.14	0.14	0.2	0.5	1	4	0.4457	0.0567
(6) Aspect	0.33	1	0.33	0.25	0.25	1	0.4353	0.0554

Table 3 -Weights assigned to the slope angle and slope aspect parameters.

Slope angle [°]	Factor weight	Slope aspect	Factor weight
0°-10°	0.1	N	0.2
11°-20°	0.4	NE	0.4
21°-30°	0.8	E	0.6
31°-40°	1	SE	0.8
41°-50°	0.6	S	1
51°-60°	0.2	SW	0.8
61°-70°	0.1	W	0.6
>70°	0.1	NW	0.4

Table 4 - Weights assigned to the distance from lineament, distance from drainage net and plan curvature parameters.

Distance from lineament (m)	Factor weight	Distance from drainage net (m)	Factor weight	Plan curvature	Factor weight
0-50	0.7	0-50	0.7	Hollows	0.8
50-100	0.2	50-100	0.2	Noses	0.1
>100	0.1	>100	0.1	Planar regions	0.3

Table 5 - Weights assigned to geological formations and quaternary deposits parameters.

Geological description	Acronym	Factor weight
Active scree and elluvium	Ez	0.9
Highest terrasse	Fx	0.9
Quaternary deposit	Fy	0.8
Lowest terrasse	Fz	0.8
Hummocky moraine	GvH	0.6
Askor amphibolite	aA	0.2
Iskere gneiss (predominantly orthogneiss)	csiUi	0.2
Stak gneiss (predominantly paragneiss)	csis	0.1
Dainyor and Thowar heterogeneous diorite	dD	0.3
Marble	mKK	0.4
Amphibolite	mdD	0.4
Sulfide and sulphur mineralization	s	0.2
Dobani - Dasu ultramafics	sD	0.1
Bilchar tonalite to granodiorite - Skoyo tonalite	tB	0.1
N-Barti tonalite to granodiorite	tgdB	0.2
Chalt formation and Turmik greenstone group	vsC	0.5
Sinakkar volcano-sediment	vsS	0.7

Table 6 - Main landslide surveyed and outlined in the Bagrot valley area using the I.F.F.I. methodological approach [APAT, 2005].

ID number	Type of landslide	Area (km²)	State of activity
B_001	Rock fall	1.94	Active
B_002	Area subjected to rock fall phenomena	13.94	Active
B_003	Rock fall	1.07	Active
B_004	Debris flow	11.87	Active
B_005	Debris flow	6.06	Dormant
B_006	Rock fall	2.54	Dormant
B_007	Debris flow	1.26	Active
B_008	Debris flow	0.82	Dormant
B_009	Debris flow	0.93	Active
B_010	Debris flow	2.13	Active
B_011	Rock fall	2.19	Active
B_012	Debris flow	0.93	Active
B_013	Debris flow	0.27	Active
B_014	Area subjected to rock fall phenomena	5.98	Active
B_015	Area subjected to rock fall phenomena	2.31	Active

Geological setting

In the area of CKNP, the geology is mainly influenced by the presence of regional tectonic structures, as the Bagrot valley area is close to the Main Karakoram Thrust (MKT), the Raikot Fault and the Main Mantle Trust (MMT). During the field survey, 3 NW-SE oriented faults were identified in the southern part of the valley (Fig. 2). The geology of the investigated area and the lineaments showing fractures, discontinuities, and shear zones were derived from the Geological Map of Hunza to Baltistan Karakoram – Koisthan – Ladakh – Himalaya North Pakistan realized by Le Fort and Pecher in 2002 at 1:150,000 scale [Le Fort et al., 2002].

In the Bagrot area the formations that mainly outcrop are belonging to the Chalt Group (vsC), a group made by volcanic and sedimentary rocks. In the central part of the valley intrusive rocks of the Kohistan –Ladahk arc of the North of the Dobani – Dasu ultramafics Formation, are present. The Sinakkar volcano sediments are found in the southern side of the valley where is also possible to identify amphibolites of the Askor Formation, Dainyor diorites and Bilchar tonalite to granodiorite of the South of the Dobani – Dasu ultramafics Formation.

All of the outcropping rocks are folded, faulted, and sheared to varying degrees, and they have been subjected to high levels of weathering and erosion.

Digital Elevation Model and its derivatives

The research used, as topographical base, the maps derived from the high-spatial-resolution multispectral images known as ASTER images. The Advanced Spaceborne Thermal Emission and Reflection Radiometer (ASTER) on NASA's Terra spacecraft collects in-track stereo using nadir- and aft looking near infrared cameras.
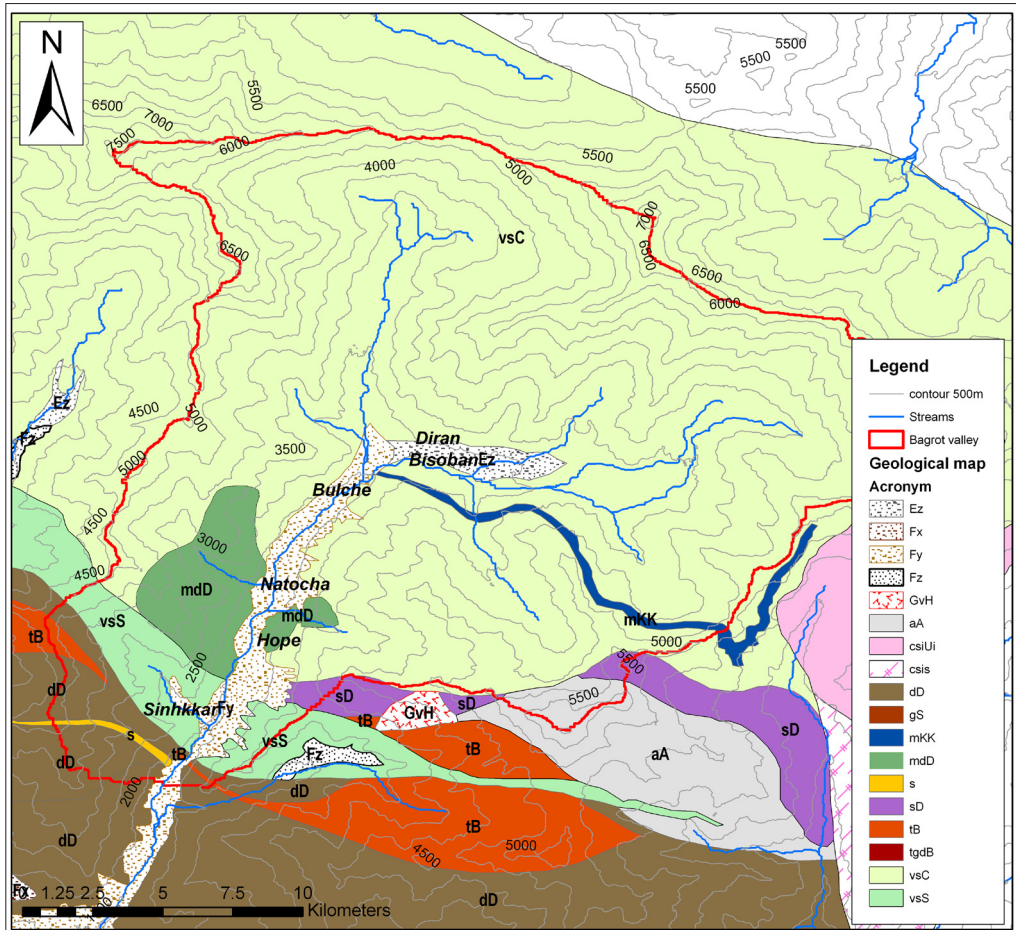
Figure 2 - Extract of geological map at 1:150,000 scale for the Bagrot valley area [Le Fort et al., 2002].

Since 2000, these stereo pairs have been used to produce single-scene (60 x 60 km) DEM at resolution of 30 m, having vertical accuracies (RMSE) generally between 10 m and 25 m. On June 29, 2009, NASA and the Ministry of Economy, Trade and Industry (METI) of Japan released a Global Digital Elevation Model (GDEM) for users worldwide at no charge, as a contribution to the Global Earth Observing System of Systems (GEOSS). NASA and METI have released a second version of the ASTER GDEM (GDEM2) in mid-October, 2011. The GDEM2 has the same gridding and tile structure as GDEM1, but benefits from the inclusion of 260,000 additional scenes to improve coverage, a smaller correlation kernel (5x5 versus 9x9 for GDEM1) yielding higher spatial resolution, and improved water masking. While the ASTER GDEM2 benefits from substantial improvements over GDEM1, users are nonetheless advised that the products may still contain anomalies and artifacts that will reduce its usability for certain applications, because they may introduce large elevation errors on local scales. The GDEM2 used in this research was acquired by downloading it from http://reverb.echo.nasa.gov/reverb with the bounding box of the Northern Areas limit.

With reference to the limitation expressed above, a comparison between the GDEM1 and GDEM2 datasets on CKNP has been done. The main problem in GDEM1 was the lack of data on some of the peaks due probably to the high reflectance of snow and ice. This mistake in GDEM2 has been corrected.

The resulted DEM presents some artifacts visible as a regular grid that may produce irregular data in the derived maps. The minimization of this noise was resolved with the application of a neighborhood operation that computes an output raster where the value for each output cell is a function of the values of all the input cells that are in a specified neighborhood around that location. A kernel of 5x5 was chosen and the mean was calculated for the output pixel.

Geomorphometric analysis: slope, aspect and curvature parameters

From ASTER DEM three different topographic attributes such as slope angle, aspect and plan curvature have been derived. These consist in the first step to describe the geomorphologic landforms and processes [Chang and Tsai, 1991; Ohlmacher, 2007].

The slope was divided into 8 classes [Ruff et al., 2008], from 0° to more than 75°. It is known that likely highest susceptibility consists in slope angles between 20 and 40° [Ruff et al., 2008]. Rock falls are instead the main type of mass movement at higher angles.

The aspect parameters is linked to the solar insolation and to the vegetation: on the solar insolation degree rocks are subjected to a differential surface degradation and to a consequent different behavior; the type and quantity of vegetation present in an area, is also linked to the slope orientation and to the roots characteristics that are weakening the surface geotechnical characteristics of the interested rocks. Eight classes characterize the aspect value, which may be used as an indicator for valley asymmetries. Southward orientations imply a high susceptibility for soil slides. As defined by Ruff et al. [2008], a high susceptibility weight was given to the southward orientated slopes and medium to low weights were assigned symmetrically to the other directions.

The surface curvature was found to be an optimal topographic attribute for the analysis for any geomorphic signatures of a surface. Olmacher [2007], Tarolli et al. [2012], and Lin et al. [2013], used it to better characterize and then analyze the geomorphology of landslide scars. Different methods have also been proposed in literature for the calculation of the various terrain parameters [e.g. Travis et al., 1975; Horn, 1981; Zevenbergen and Thorne, 1987]. In this work we used the curvature derived by the fourth-order polynomial proposed by Zevenbergen and Thorne [1987]; in detail we considered the curvature of the surface perpendicular to the slope direction (plan curvature). The plan curvature noses and hollows may be quite easily identified due to their very complex and divergent profiles. Mesoscale objects such as wide debris flow fans may be identified with the plan curvature map. For this reason, in the present research the plan curvature map has been calculated for the Bagrot valley area.

Landslide distribution map

Landslides were identified using DEM hillshade data set and the curvature map derived from the DEM. Due to the lack of vegetation, a high reflectance is present and the identification of the phenomena is easier. All of the mapped landslides were later cross-checked in the field.

In this area most of the landslides are represented by rock falls, debris falls and debris flows (Fig. 3). No rotational or translational slides were identified during the field survey. The rock falls are widely distributed although the valley, along both sides, where is possible to identify

coalescing debris fans (Fig. 3). Steep cliffs are heavily subjected to physical weathering having as a consequence a decrease in the geotechnical characteristics and an accelerated weakening of the rocks creating daily rock falls. Areas subjected to rock falls have a maximum length of 6.4 km with a height difference of 2000 m in some places. One of the smallest phenomena has a scree extension of about 1 km. All the Bagrot valley area is interested by active rock falls, only some small portions of the surveyed territory may be considered as not subjected to these phenomena. In addition, most of the debris flows are active. In this region, villages are built on the debris flow stabilized fans where the gentle slope defines a wide cultivable area. The active channel of the debris flow usually remains on one side of the cultivated fan. The smaller debris phenomena may be instead considered active. These are locations of avalanches and/or debris flows during the different seasons (Tab. 6).

Debris falls are common features observed in these areas, where terraces are heavily interested by them. The heights of the terraces may reach 100 m, and the toe erosion is their main triggering cause. The most part of surveyed landslides may be considered active according to the WP/WLI Multilingual Landslide Glossary [UNESCO, 1993].
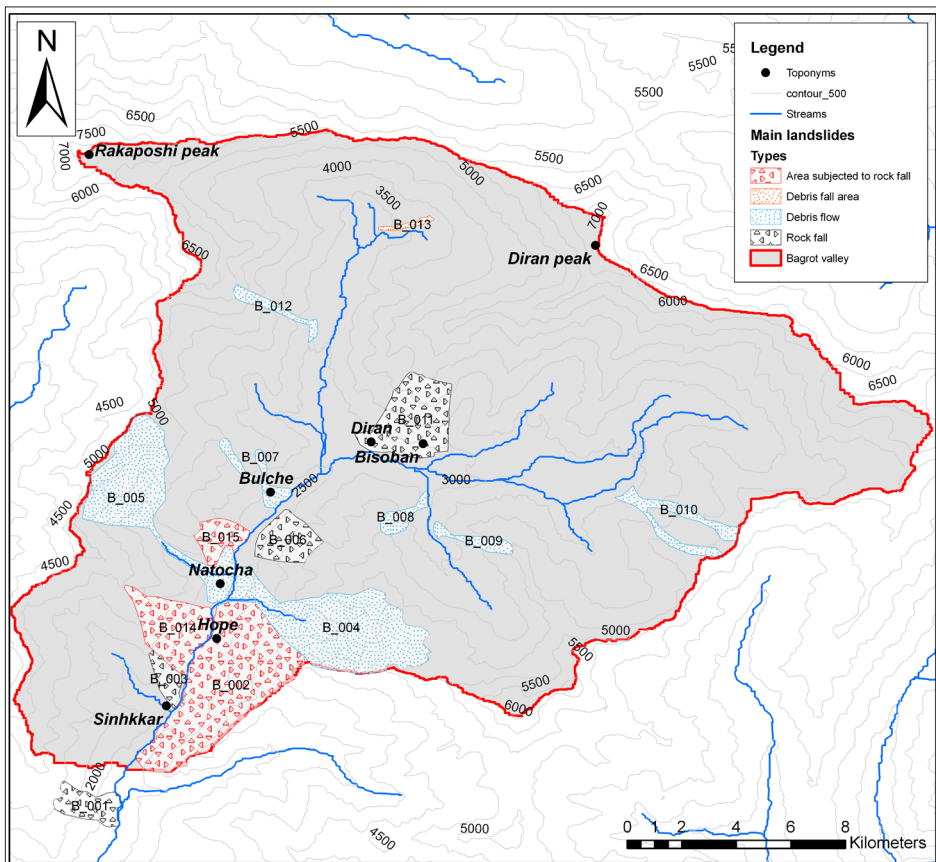

Figure 3 - Main landslides identified in the Bagrot valley area; landslide perimeter has been realized following the I.F.F.I. proposed methodology [ISPRA, 2012].

Results and discussion

Knowing that a simple pair-wise comparison in which only two parameters may be considered at a time means simplifying the weighting process and making it more opinion-based dependent, but the method guarantees a widespread superficial knowledge of the wild territories also with few parameters.

During the field work in the Bagrot valley area, mainly rock falls and debris flows were identified and this predominance has been highlighted also by the parameter analysis through the GIS tools. The scale of the available geological map (1:150,000) and the cell size (30 m) did not permit to obtain a detailed map, but guaranteed a wide geomorphological analysis.

The influence of the fault/lineament parameter was considered and simulated creating buffer zones around the fault lines (0-50 m, 50-100 m and more than 100 m). These distances were decided according to the field survey evidences showing that faults are not equally distributed. The same subdivision was assigned also to the distance to stream parameter. Landslides may occur on the sides of the slopes affected by streams. In the studied area, the proximity to streams is an important parameter considered the erosion capacity of the flowing waters in such a barren territory especially during monsoon season.

The importance of the aspect parameter was based on the landslide distribution. According to Dhakal, south- and east-facing slopes were considered to be more susceptible for landslides [Dhakal et al., 2000].

The land use parameter, during this first screening analysis, was not considered. Barren slopes are widespread and the vegetation is mainly confined to the valley floors, where the slope angles are more gentle (< 15°). Hence, in a first approximation, the parameter was considered to have the same influence/value all over the investigated area. For future analyses, to obtain more reliable results, land use and land cover parameters will be taken into account.

To obtain the landslide susceptibility map, as previously defined, parameters were weighted and a WLC was obtained producing a continuous scale of numerical values (LI). These values were later divided into six susceptibility classes using the standard deviation [Ayalev et al., 2004]. These categories are described in Table 7 and correspond to six relative scales of landslide susceptibility (Fig. 4).

Table 7 - Susceptibility classes.

Classes	N. of cells	%	Susceptibility description
1	647	0.13	Extremly low susceptible
2	46760	9.71	Very low susceptible
3	107003	22.22	Low susceptible
4	160054	33.25	Medium susceptible
5	133666	27.76	High susceptible
6	33246	6.91	Very high susceptible

Medium (33.25%) and high (27.76%) are the most populated categories corresponding to areas were the slope gradient is elevated and the plan curvature is hollow. This demonstrates the importance of the weight of these 2 parameters. Also geology and distance to structural lineaments played an important role; weaker rocks are more prone to fall. While, as

expected, flat areas, as the ones covered by glaciers, resulted to be more stable. These last ones are covering an area of 0.13% (extremely low susceptibility) or very low as for the 9.71% of the territory. Only the 6.91% is instead characterized by a very high susceptibility: these areas are the ones where the terraces are present (loose material eroded at the toe by the rivers, are creating impressive collapsing of material) or steep slopes where rock falls are the main recognized phenomena. The percentage obtained trough the analysis are macroscopically describing, trough the numbers, the existing real situation recognized during the field survey and characteristic of the Himalayan - Karakoram environment.
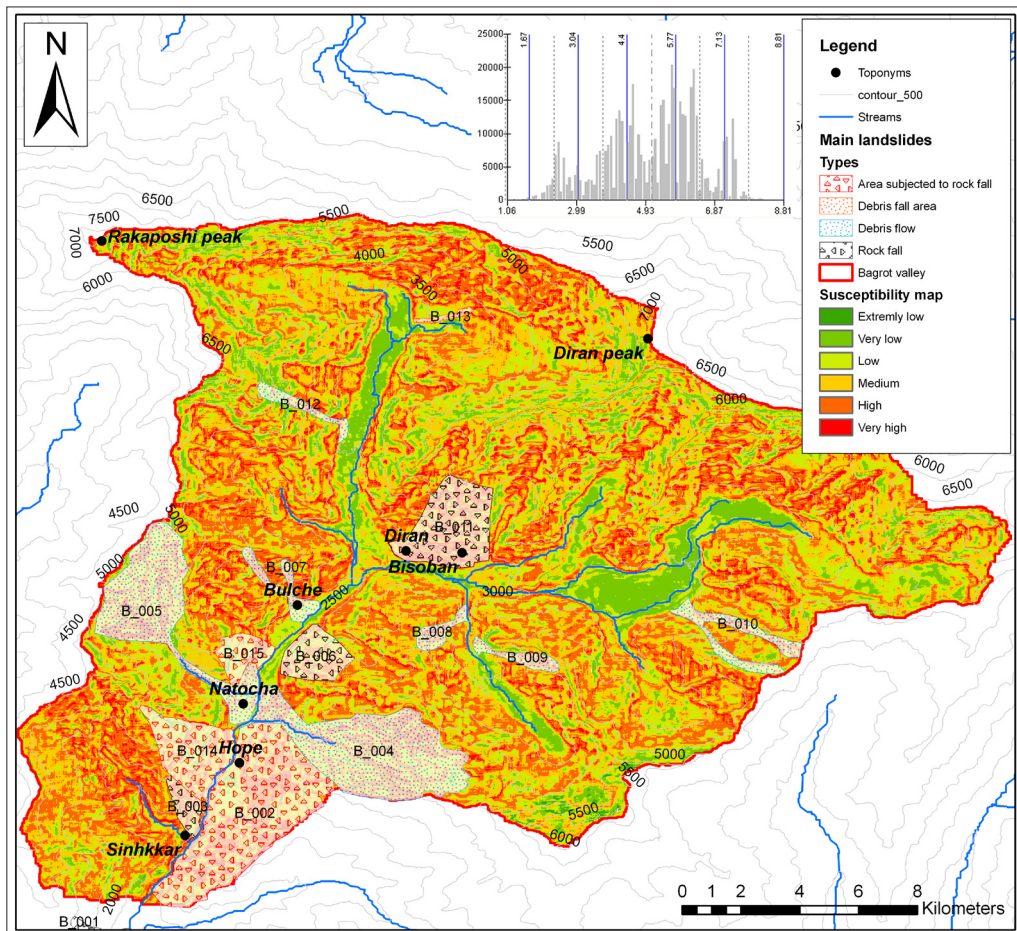

Figure 4 - Landslide susceptibility map obtained for the Bagrot valley area. Susceptibility has been classified into 6 classes by the standard deviation method modifying Ayalev, 2004.

Conclusions

The simple methodology presented in this work permits to define the areas which have an intrinsic susceptibility to landslides. The methodology belongs to the generation of maps obtained through the weighted overlay of different data layers.

In this study 6 event-controlling parameters namely geology, aspect, slope, distance from drainage, distance from lineaments and plan curvature were considered. Their interaction with the analytical hierarchy process and the Weighed Linear Combination permitted to obtain a landslide susceptibility map. The result of the entire analysis was that the investigated area was divided into 6 classes of susceptibility: extremely low (0.13%), very low (9.71%), low (22.22%), medium (33.25%), high (27.76%) and very high (6.91%).

The quality of these results heavily depends on the quality of the input data, but the methodological approach is so simple that it may be easily upgraded on demand and it provides a relatively quick analysis. So it may be considered a useful tool to identify slope sectors liable to landsliding.

The research has obvious limits due to the scale of the available geological map (1:150,000), the resolution of the ASTER DEM (30 m x 30 m), the lack of some fundamental information such as the land use or top soil cover, but it is just the beginning of a multi-disciplinary study in which different themes are going to converge during the following years. The other research units involved in the SEED project are working on themes that will be included in the landslide susceptibility analysis as land and ice covers. These aims will be reached at the end of 2013. Besides, in the meantime, a request has been realized to obtain more detailed DEMs for some specific areas that will permit to reach a more reliable result also in areas where data are not always available and easy to obtain.

Acknowledgements

References

Abrams M. (2000) - *The Advanced Spaceborne Thermal Emission and Reflection Radiometer (ASTER): data products for the high spatial resolution imager on NASA's Terra platform*. International Journal of Remote Sensing, 21: 847-859. doi: http://dx.doi.org/10.1080/014311600210326.

Ansari Z. R., Rao L.A.K., Saran Sameer (2012) - *Comparative Study of Terrain Elements from Different DEMs*. International Journal of Remote Sensing and GIS, 1 (2): 57-76. ISSN 2277-9051.

Ayalew L., Yamagishi H., Ugawa N. (2004) - *Landslide susceptibility mapping using GIS-based weighted linear combination, the case in Tsugawa area of Agano River, Niigata Prefecture, Japan*. Landslides, 1:73-81. doi: http://dx.doi.org/10.1007/s10346-003-0006-9.

Bajracharya B., Bajracharya S.R. (2008) - *Landslide mapping of the Everest region using high resolution satellite images and 3D visualization*. Mountain GIS eConference. Available at: http://www.mtnforum.org/sites/default/files/pub/landslide.pdf. (last accessed: 15/05/2012).

Bubenzer O., Bolten A. (2008) - *The use of new elevation data (SRTM/ASTER) for the detection and morphometric quantification of Pleistocene megadunes (draa) in the*

eastern Sahara and the southern Namib. Geomorphology, 102: 221-231. doi: http://dx.doi.org/10.1016/j.geomorph.2008.05.003.

Chang K., Tsai B. (1991) - *The Effect of DEM Resolution on Slope and Aspect Mapping*. Cartography and Geographic Information Systems, 18 (1): 69-77. doi: http://dx.doi.org/10.1559/152304091783805626.

Chacon J., Irigaray C., Fernandez T., El Hamdouni R. (2006) - *Engineering geology maps: landslides and geographical information systems*. Bulletin Engineering Geology and Environment, 65: 341-411. doi: http://dx.doi.org/10.1007/s10064-006-0064-z.

Chau K.T., Sze Y.L., Fung M.K., Wong W.Y., Fong E.L., Chan L.C.P. (2004) - *Landslide hazard analysis for Hong Kong using landslide inventory and GIS*. Computers & Geosciences, 30 (4): 429-443. doi: http://dx.doi.org/10.1016/j.cageo.2003.08.013.

Choi J., Oh H., Lee H.J., Lee C., Lee S. (2012) - *Combining landslide susceptibility maps obtained from frequency ratio, logistic regression, and artificial neural network models using ASTER images and GIS*. Engineering Geology, 124: 12-23. doi: http://dx.doi.org/10.1016/j.enggeo.2011.09.011.

Dahal R.K., Hasegawa S., Nonomura A., Yamanaka M., Masuda T., Nishino K. (2008) - *GIS-based weights-of-evidence modeling of rainfall-induced landslides in small catchments for landslide susceptibility mapping*. Environmental Geology, 54 (2): 314-324. doi: http://dx.doi.org/10.1007/s00254-007-0818-3.

Dhakal A.S., Amada T., Aniya M. (2000) - *Landslide hazard mapping and its evaluation using GIS: an investigation of sampling schemes for a grid-cell based quantitative method*. Photogrammetric Engineering and Remote Sensing, 66 (8): 981-989.

Davis J. (1986) - *Statistics and data analysis in geology*. John Wiley & Sons, New York, N.Y., pp. 646.

EV-K2-CNR Committee (2008) - Seed Context. Available at: http://www.evk2cnr.org/cms/en/research/integrated_programs/seed/context. (last accessed: 08/02/2012).

Fell R., Corominas J., Bonnard C., Cascini L., Leroi E., Savage W. (2008) – Guidelines for landslide susceptibility, hazard and risk zoning for land use-planning. Engineering Geology, 102: 99-111. doi: http://dx.doi.org/10.1016/j.enggeo.2008.03.014.

Fourniadis I.G., Liu J.G., Mason P.J. (2007) - *Landslide hazard assessment in the Three Gorges area, China, using ASTER imagery: Wushan–Badong*. Geomorphology, 84: 126-144. doi: http://dx.doi.org/10.1016/j.geomorph.2006.07.020.

Gardner J.S., Saczuk E. (2004) - *System for hazard identification in High Mountain Areas: An example from the Kullu District, Western Himalaya*. Journal of Mountain Science, 1 (2): 115-127. doi: http://dx.doi.org/10.1007/BF02919334.

Gokceoglu C. (2012) - *Discussion on "Combining landslide susceptibility maps obtained from frequency ratio, logistic regression, and artificial neural network models using ASTER images and GIS" by Choi et al. (2012), Engineering Geology, 124: 12-23*. Engineering Geology, 129-130,104 (2). ISSN: 0013-7952.

Gullà G., Antronico L., Iaquinta P., Terranova O. (2008) - *Susceptibility and triggering scenarios at regional scale for shallow landslides*. Geomorphology, 99: 39-58. doi: http://dx.doi.org/10.1016/j.geomorph.2007.10.005.

Guzzetti F., Mondini A.C., Cardinali M., Fiorucci F., Santangelo M., Chang K.T. (2012) - Landslide inventory maps: New tools for an old problem. Earth-Science Reviews, 112: 42-66. doi: http://dx.doi.org/10.1016/j.earscirev.2012.02.001.

Horn BKP. (1981) - *Hill shading and the reflectance map*. Proceedings of the IEEE, 69 (1): 14-47. doi: http://dx.doi.org/10.1109/PROC.1981.11918.

Intarawichian N., Dasanada S. (2010) - *Analytical Hierarchy Process for landslide susceptibility mapping in lower Mae Chaem watershed, northern Thailand. Suranaree*. Journal of Science Technology, 17 (3): 227-292.

ISPRA (2012) - *I.F.F.I. Project*. Available at: http://193.206.192.136/cartanetiffi/default_nosso.asp. (last accessed: 20/09/2012).

Kamp U., Bolch T., Olsenholler J. (2003) - *DEM generation from ASTER satellite data for geomorphometric analysis of cerro sillajhuay, Chile/Bolivia*. Proceedings of the ASPRS 2003 Annual Conference. Anchorage, Alaska, USA, pp. 9.

Kamp U., Growley B. J., Khattak G.A., Owen L.A. (2008) - *GIS-based landslide susceptibility mapping for the 2005 Kashmir earthquake region*. Geomorphology, 101: 631-642. doi: http://dx.doi.org/10.1016/j.geomorph.2008.03.003.

Kawabata, D., Bandibas J. (2009) - *Landslide susceptibility mapping using geological data, a DEM from ASTER images and an Artificial Neural Network (ANN)*. Geomorphology, 113 (1-2): 97-109. doi: http://dx.doi.org/10.1016/j.geomorph.2009.06.006.

Komac M. (2006) - *A landslide susceptibility model using the Analytical Hierarchy Process method and multivariate statistics in perialpine Slovenia*. Geomorphology, 74: 17-28. doi: http://dx.doi.org/10.1016/j.geomorph.2005.07.005.

Le Fort P., Arnaud P. (2002) - *Geological Map of Hunza to Baltistan Karakoram - Koisthan - Ladakh - Himalaya North Pakistan (1:150,000 scale)*. Geologica, 6 (1): 1-199. ISSN: 1025-2541.

Lin C.W., Tseng C.-M., Tseng Y.-H., Fei L.-Y., Hsieh Y.-C., Tarolli P. (2013) - *Recognition of large scale deep-seated landslides in forest areas of Taiwan using high resolution topography*. Journal of Asian Earth Sciences, 62: 389-400. doi: http://dx.doi.org/10.1016/j.jseaes.2012.10.022.

Moradi M., Bazyar M.H., Mohammadi Z. (2012) - *GIS-based landslide susceptibility mapping by AHP method, a case study, Dena city, Iran*. Journal of Basic and Applied Scientific Research, 2 (7): 6715-6723. ISSN 2090-4304.

Nefeslioglu H.A., Gokceoglu C., Sonmez H. (2008) - *An assessment on the use of logistic regression and artificial neural networks with different sampling strategies for the preparation of landslide susceptibility maps*. Engineering Geology, 97 (3-4): 171-191. doi: http://dx.doi.org/10.1016/j.enggeo.2008.01.004.

Ohlmacher G.C. (2007) - *Plan curvature and landslide probability in regions dominated by earth flows and earth slides*. Engineering Geology, 91: 117-134. doi: http://dx.doi.org/10.1016/j.enggeo.2007.01.005.

Othman N.A., Naim W.M., Noraini S. (2012) - *GIS based multi-criteria decision making for landslide hazard zonation*. Procedia - Social and Behavioral Sciences, 35: 595-602.

Peduzzi P. (2010) - *Landslides and vegetation cover in the 2005 North Pakistan earthquake: a GIS and statistical quantitative approach*. Natural Hazards Earth System Science, 10: 623-640. doi: http://dx.doi.org/10.5194/nhess-10-623-2010.

Phukon P., Chetia D., Das P. (2012) - *Landslide Susceptibility Assessment in the Guwahati City, Assam using Analytic Hierarchy Process (AHP) and Geographic Information System (GIS)*. International Journal of Computer Applications in Engineering Sciences, 2 (1). ISSN: 2231-4946.

Ruff M., Czurda K. (2008) - *Landslide susceptibility analysis with a heuristic approach in the Eastern Alps (Vorarlberg, Austria)*. Geomorphology, 94: 314-324. doi: http://dx.doi.org/10.1016/j.geomorph.2006.10.032.

Saaty T.L. (2000) - *The Analytic Hierarchy Process*. Mc Graw Hill, 1980.

Sarkar S., Kanungo D.P. (2004) - *An integrated approach for landslide susceptibility mapping using remote sensing and GIS*. Photogrammetric engineering and remote sensing, 70 (5): 617-625.

Song K.Y., Oh H.J., Choi J., Park I., Lee C., Lee S. (2012) - *Prediction of landslide using ASTER imagery and data mining models*. Advanced Space Resolution, 49: 978-993. doi: http://dx.doi.org/10.1016/j.asr.2011.11.035.

Spiker E.C., Gori P.L. (2000) - *National landslide hazards mitigation strategy: a framework for loss reduction*. Department of Interior, USGS, Open-file Report 00-450, 49.

Tarolli P., Arrowsmith J.R., Vivoni E.R. (2009) - *Understanding earth surface processes from remotely sensed digital terrain models*. Geomorphology, 113: 1-3. ISSN: 0169-555X. doi: http://dx.doi.org/10.1016/j.geomorph.2009.07.005.

Tarolli P., Sofia G., Dalla Fontana G. (2012) - *Geomorphic features extraction from high resolution topography: landslide crowns and bank erosion*. Natural Hazards, 61: 65-83. doi: http://dx.doi.org/10.1007/s11069-010-9695-2.

Toutin T. (2008) - *ASTER DEMs for geomatic and geoscientific applications: a review*. International Journal of Remote Sensing, 29 (7):1855-1875. doi: http://dx.doi.org/10.1080/01431160701408477.

Travis M.R., Elsner G.H., Iverson W.D., Johnson C.G. (1975) - *VIEWIT Computation of Seen Areas, Slope and Aspect for Land Use Planning*. PSW 11/1975, Pacific Southwest Forest and Range Experimental Station, Berkeley, California, USA.

UNESCO (1993) - *Multilingual landslide glossary. The International Geotechnical Societes*. UNESCO Working party for world landslide inventory. BiTech Publishers. Canada. ISBN 0-920 505-10-4.

Van Wasten C.J., Castellanos E., Kuriakose S.L. (2008) - *Spatial data for landslide susceptibility, hazard and vulnerability assessment: an overview*. Engineering Geology, 102 (3-4): 121-131.

Varnes D.J. (1984) - *Landslide hazard zonation: a review of principles and practice*. Commission on landslides of the IAEG, UNESCO. Natural Hazards, 3: 61.

Zevenbergen L.W., Thorne C. (1987) - *Quantitative analysis of land surface topography*. Earth Surface Processes and Landforms, 12: 47-56. doi: http://dx.doi.org/10.1002/esp.3290120107.